Sodium Variable Conductance Heat Pipe for Radioisotope Stirling Systems

Calin Tarau[1], William G. Anderson[2], and Kara Walker[3]
Advanced Cooling Technologies, Inc., Lancaster, PA, 17601 U.S.A.

In a Stirling radioisotope system, heat must continually be removed from the General Purpose Heat Source (GPHS) modules to maintain the modules and surrounding insulation at acceptable temperatures. Normally, the Stirling convertor provides this cooling. If the convertor stops in the current system, the insulation is designed to spoil, preventing damage to the GPHS, and also ending the mission. An alkali-metal Variable Conductance Heat Pipe (VCHP) has been designed to allow multiple stops and restarts of the Stirling convertor in an Advanced Stirling Radioisotope Generator (ASRG). When the Stirling convertor is turned off, the VCHP will activate when the temperatures rises 30°C above the set point temperature. A prototype VCHP with sodium as the working fluid was fabricated and tested in both "gravity aided" and "against gravity" conditions for a nominal heater head temperature of 790ºC. The results show very good agreement with the predictions and validate the model. The gas front was located at the exit of the evaporator when heater head temperature was 790ºC while cooling was ON, simulating an operating Advanced Stirling Convertor (ASC). When cooling stopped, the temperature increased by 30°C, allowing the gas front to move past the radiator, which transferred the heat to the case. After resuming the cooling flow, the front returned at the initial location turning OFF the VCHP. The "against gravity" working conditions showed a colder reservoir and faster transients.

I. Introduction

IN a Stirling radioisotope power system, one or more General Purpose Heat Source (GPHS) modules supply heat to a Stirling convertor (Stirling engine with an integrated linear alternator). This heat is used to generate electric power, while the waste heat is radiated to space. The maximum allowable GPHS module operating temperature is set by the iridium cladding around the fuel. The GPHS module is designed so that it will not release radioisotopes, even under such postulated events as a launch vehicle explosion, or reentry through the earth's atmosphere. However, if the iridium cladding was to overheat, grain boundary growth could weaken the cladding, possibly allowing radioisotopes to be released during an accident. Once the GPHS is installed in the radioisotope Stirling system, it must be continually cooled. Normally, the Stirling convertor removes the heat, keeping the GPHS modules cool. There are three basic times when it may be desirable to stop and restart the Stirling convertor:

1) During installation of the GPHS
2) During some missions when taking scientific measurements to minimize electromagnetic interference and vibration
3) Any unexpected stoppage of the convertor during operation on the ground or during a mission.

In the current system, the insulation will spoil to protect the GPHS from overheating. A VCHP would allow convertor operation to be restarted on a planned convertor stoppage and potentially allow for convertor restart on any unexpected stoppage, depending on the reason for the stoppage. It would also save replacing the insulation after such an event during ground testing.

---

[1] R&D Engineer, Aerospace Products.
[2] Lead Engineer, Aerospace Products, AIAA member. Bill.Anderson@1-act.com.
[3] R&D Engineer, Aerospace Products.

A. VCHP Provides Back Up Cooling for the Stirling Radioisotope Power System

The schematics in Fig. 1 show the basic concept of the VCHP integrated with a Stirling engine. A GPHS module supplies heat to the heat collector which, in turn, wraps around the hot end of the Stirling engine's heater head, so the normal heat flow path is GPHS - heat collector - heater head. The annular evaporator of the VCHP wraps around the heat collector so, during normal operation, vapor is approximately at the heater head's temperature. The non-condensable gas (NCG) charge in the system is sized so the radiator is blocked during normal operation (see Fig. 1(a)). When the Stirling engine is stopped, the temperature of the entire system starts to increase. Since the system is saturated, the working fluid vapor pressure increases as the temperature increases. This compresses the NCG. As shown in Fig. 1b, this opens up the radiator. Once the radiator is fully open, all of the heat is dumped to the radiator, and the temperature stabilizes. Once the Stirling engine starts operating again, the vapor temperature and pressure start to drop. The non-condensable gas blankets the radiator, and the system is back to the normal state (Fig. 1(a)).

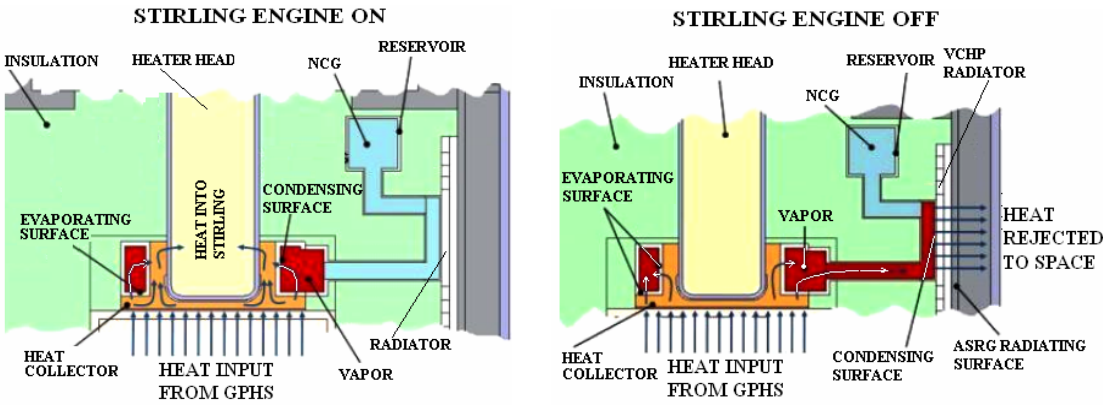

a) **b)**

Figure 1. a) VCHP delivers heat to the heater head when the Stirling engine is working. b) VCHP dumps heat to the radiator when the Stirling engine is stopped.

B. Base Line Design

The Advanced Stirling Radioisotope Generator (ASRG)[1], with an 850°C heater head temperature, was selected as the baseline design. The system consists of two Advanced Stirling Convertors (ASCs), mounted back to back for dynamic balance. Heat to each ASC is supplied by one GPHS module. During operation, a heat collector is used to conduct the heat from the GPHS into the Stirling heater head, see Fig. 2(a). A copper-based cold-side adapter flange (CSAF), shown in Fig. 2(b), is used to conduct the waste heat from the Stirling convertor cold side to the ASRG housing, where it radiates to space. The CSAF also serves as a structural member. The cold-end flange temperature is primarily set by the sink temperature seen by the ASRG radiating housing, which varies from earth (including launch) environments to deep space. Its operating temperature ranges from 40 to 120°C.

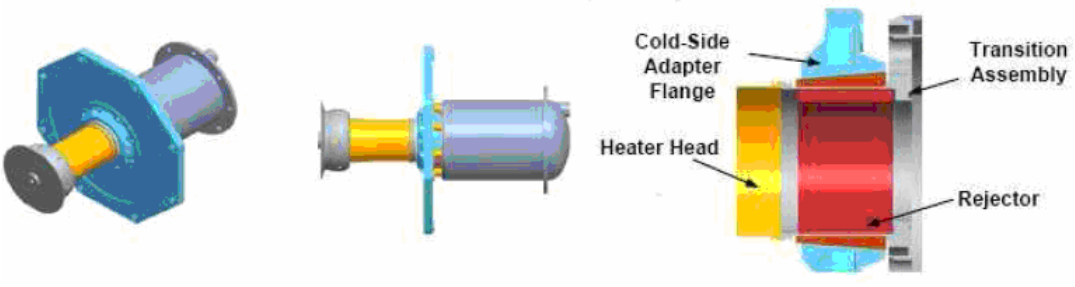

a) **b)**

Figure 2. (a) Stirling Convertor[1] with Heat Collector and Cold-Side Adapter Flange. (b) Cold-Side Adapter Flange.

C. First Prototype VCHP Design

Figure 3 is a schematic of the VCHP integrated with the ASC to provide back-up cooling. Since an ASRG consists of a pair of Stirling convertors mounted head to head, this schematic corresponds to the lower portion of

half of the ASRG system. The VCHP evaporator is wrapped around the heat collector so the original ASC configuration is not modified. The condenser is attached to the internal radiator while the reservoir is embedded inside the insulation, under the CSAF. The VCHP is designed in such a way that, during normal operation of the Stirling convertor, the working fluid vapor – NCG interface front is located at the exit of the evaporator, as far as possible from the condenser to minimize the heat losses. When the Stirling convertor is stopped, the NCG front is located at the top of the condenser, and the heat is radiated to the ASRG wall and thence into the environment.

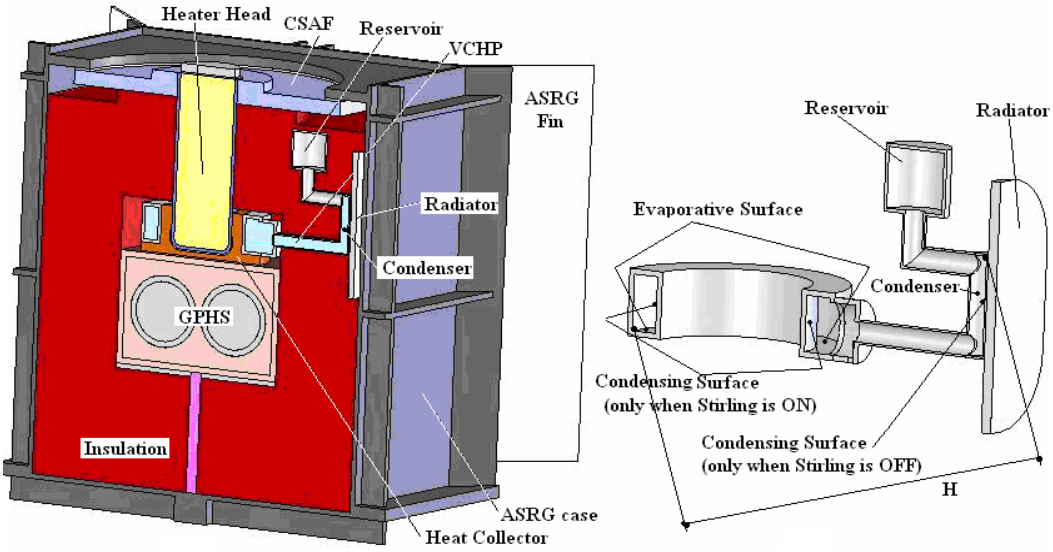

a) **b)**

Figure 3. (a) VCHP-ASRG system (b) First prototype VCHP with internal condenser and the reservoir embedded within the insulation.

The VCHP dimensions are driven by both the configuration and the wick design. Three wraps of SS 100 x 100 stainless steel screen are used "as the wick" everywhere within the VCHP. Relevant parameters regarding the design and the fabricated first prototype VCHP are presented below in Table 1.

Table 1. First prototype VCHP physical and geometrical parameters.

	Parameter	Value
General	Material	SS304
	Number of moles of NCG (Ar) [moles]	0.00025
	Mass [g]	302
Evaporator	I.D. minimum (it matches the heat collector OD) [inch]	1.87
	O.D. maximum (external diameter) [inch]	2.75
	Height (inside) [inch]	0.741
Section between Evaporator and Condenser	Total length [inch]	1.82
	I.D. [inch]	0.256
Condenser	I.D. [inch]	0.35
	Length [inch]	1.2
Radiator	Material	Nickel
	Area [inch^2]	11
	Thickness [inch]	0.3
	Emissivity	0.85
	Fin Efficiency	0.54
Section between Condenser and Reservoir	Total length [inch]	3.65
	ID [inch]	0.256
Reservoir	Volume [inch^3]	1.285

Table 2. Capillary pumping capability and pressure drops (Pa) for the design at T_{max}=880°C.

Design Stage	Capillary Pressure	Total Pressure Drop	Gravity Head	Liquid Pressure Drop	Vapor Pressure Drop
New Design	1872	1119	848	222	48.9

Pressure drops along the VCHP are presented in Table 2, for sodium working fluid at the maximum vapor temperature of 880°C (1153K), when the VCHP is active. The total pressure drop (the sum of the three main components, due to gravity and the liquid and vapor flows) is smaller than the capillary pressure. The resultant pumping capability of 1872 Pa is greater than the total pressure drop of 1119 Pa. The most dominant pressure drop component, due to gravity, was calculated for the maximum possible elevation, H=4.6 inches, that is given by to most distant points within the VCHP (dimension "H" in Fig. 3b). The VCHP is designed to operate in any orientation.

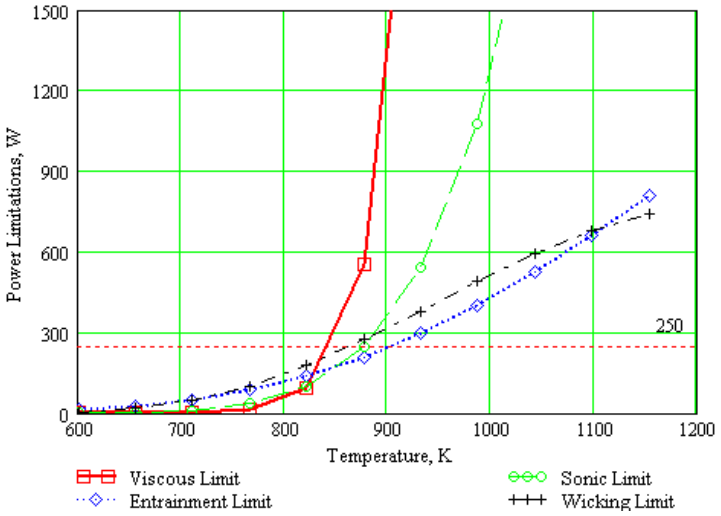

Figure 4. Performance limitations for the first VCHP prototype.

Performance limitations for the first prototype design are shown in Fig. 4. The nominal power (250 W) that the VCHP has to carry is represented with a dashed line for comparison. As expected, at lower temperatures, viscous and sonic limitations drastically restrict the pipe performance. Note that, unlike the capillary limit, these are not actually limits to the heat pipe performance. If either limit is reached with a constant heat flux source, the heat pipe temperature will increase until the limit no longer applies. At the nominal working temperature of 880°C (1153 K), the wicking limit is the most restrictive but is at much higher values than the GPHS power.

II. Experiment

The first prototype VCHP and the test setup are shown in Fig. 5. Although the material for the final VCHP will be Haynes 230 because of both its compatibility with sodium based on long duration life tests[2] and its low creep rate at 850°C, the first prototype VCHP is manufactured from stainless steel. This is mostly for convenience since it is designed to operate at lower temperature, 790°C, turning on when the vapor temperature reaches 820°C.

The "D" shaped condenser is attached to the nickel radiator through the flat surface. The nickel radiator is used for convenience in testing the first prototype, while the final VCHP will have a carbon-carbon radiator. Heat radiates from the radiator to an ASRG wall simulator, which, in turn, radiates into the ambient or to a cold wall inside the vacuum chamber.

Figure 5a shows the locations of the thermocouples used to measure the temperature distribution along the actual VCHP. Most of the thermocouples were spot welded to the pipe except thermocouples 24, 28 and 33. These thermocouples were installed into thermo-wells to measure vapor temperatures in the evaporator (TC 24 and 28) and NCG temperature in the reservoir (TC 33). Condenser temperatures are measured by thermocouples 4, 5, and 9, while radiator temperatures are measured by thermocouples 6, 7, 8, 10, 11, and 12. The remaining thermocouples, shown in Fig. 5a, measure temperature distributions along the sections between the evaporator and condenser (thermocouples 1, 2, and 3) and between the condenser and the reservoir (thermocouples 13 through 21). The average distance between the thermocouple locations was approximately 0.4 inches, except between thermocouples 24/28 and 1, where the distance was approximately 1.5 inches, and between thermocouple 21 and 33 (reservoir), where the distance was approximately 0.9 inches.

Figure 5b shows the VCHP integrated in the experimental setup. The GPHS is simulated by a $MoSi_2$ heater, which radiantly heats the bottom of the heat collector. Heat removal by the Stirling convertor is simulated by a steady flow of air that travels down the central tube, and travels up the outer tube, exiting at the top of the outer tube.

Thermocouples 22 and 26 monitor the coolant (compressed air) IN and OUT temperatures. Temperatures in the evaporating/condensing areas of the "donut" are measured in the heat collector walls by thermocouples 25, just under the evaporation interface, and 23, next to the condensation interface.

To protect the heater, the bulk of the measurements during the testing of the first prototype were made at a vapor temperature lower than the nominal 850°C. A vapor temperature of 790°C was chosen for most of the tests. In this case, for 0.00025 moles of NCG (argon) and a VCHP activation temperature difference of 30°C, the required cold and hot reservoir temperatures were 208°C and 382°C, respectively.

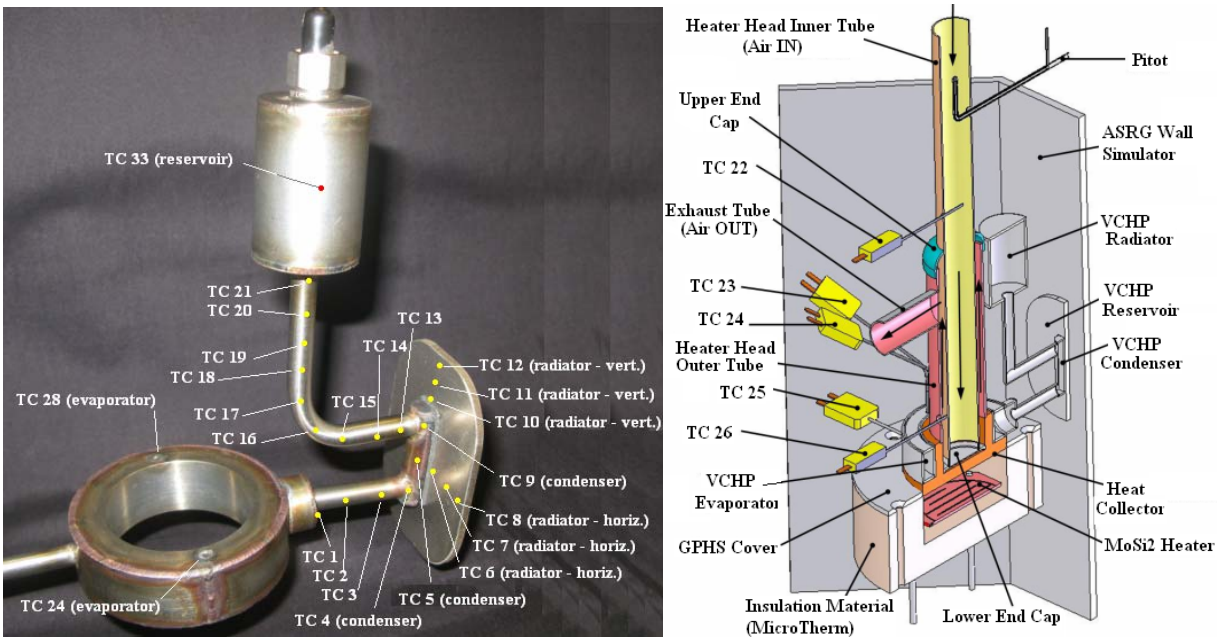

a) **b)**

Figure 5. VCHP integration with the experimental setup (a) Fabricated first prototype VCHP, (b) Test setup.

A. Preliminary Experimental Procedure and Results

A preliminary experiment with the pipe "gravity aided" (sodium can drip back from the condenser to the annular evaporator – see Fig.5) was carried out to calibrate the system. The parameters sought during calibration were:

1) Heater power
2) Coolant (air) flow rate to simulate the Stirling convertor
3) Heat loss through the insulation

These parameters were determined in three experimental sequences, A1, A2, and A3 described below.

During sequence A1, the required heater power to fully activate the VCHP radiator was determined. The heater power

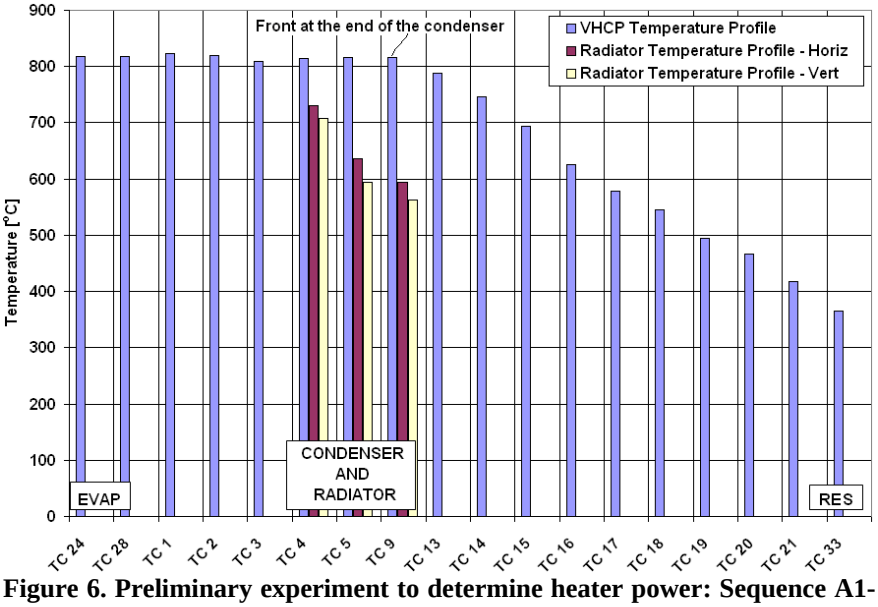

Figure 6. Preliminary experiment to determine heater power: Sequence A1- front reaches the end of the condenser with no cooling (ASC OFF), at a vapor temperature of 820°C, reservoir temperature of 373°C and a total power of 455 W.

was incrementally increased, activating the VCHP, until the front settled at the end of the condenser (TC 9), reaching steady state conditions with no cooling (simulating the ASC OFF) (see Fig. 6). The vapor temperature reached 820°C, resulting in a 30°C temperature rise above the design vapor temperature with the ASC ON (VCHP OFF) of 790°C, while the reservoir temperature was approximately 373°C (compared to a 382°C design temperature for this condition of hot reservoir and VCHP ON). The total heater power required to maintain steady state was 455W. The heater temperature was 1033°C, resulting in a 213°C temperature difference between the heater and the sodium vapor. The average radiator and radiated wall temperatures were 637°C and 95.5°C, respectively.

During sequence A2, the coolant flow rate to simulate the heat transfer in the Stirling convertor was determined. For this, the total electrical power was kept constant (at 455W), while the cooling air was started (simulating the ASC as ON) and increased in step wise increments. The flow rate was increased until the NCG front retracted and settled at the exit of the evaporator; see Fig. 7. The vapor temperature was 790°C (verifying the design condition with the ASC ON and the 30 °C temperature difference between ASC ON and ASC OFF) and the reservoir temperature was 248°C, compared to the 210°C design temperature for the cold reservoir situation (VCHP OFF). The air-cooling velocity used to maintain steady state within these parameters was 7.6 m/s. The heater temperature was 1003°C, maintaining the same temperature difference, 213°C, between the heater and the sodium vapor. The average radiator and radiated wall temperatures were 275°C and 44°C, respectively. Although thermocouples for air IN and OUT temperatures were provided for calorimetric calculations, the power carried by the coolant was not calculated because of the inaccuracy of the volumetric air flow rate as calculated from the air velocity measured by the pitot tube. Therefore, only the air velocity was considered, and it represented a reference when comparing cooling conditions from one situation to another. The value of 7.6 m/s was used throughout the remaining experiments to simulate the Stirling convertor operating (ASC ON).

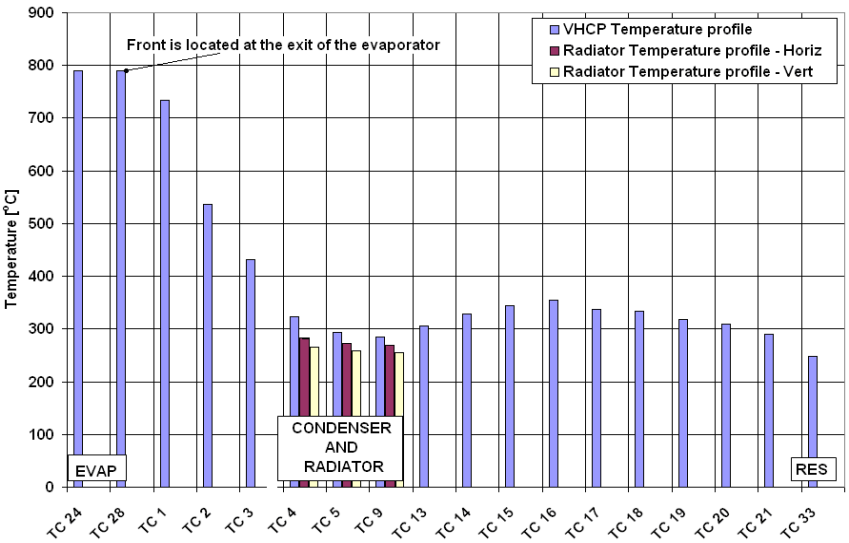

Figure 7. Preliminary experiment: Sequence A2 - front settles at the exit of the evaporator at a vapor temperature of 790°C, reservoir temperature of 248°C, total applied power of 455 W and air cooling at 7.6 m/s (ASC ON).

During sequence A3, heat losses through the insulation were evaluated. Total heater power and air velocity were simultaneously decreased, while maintaining the vapor at a constant temperature of 790°C. With no air flow, a power of 162 W was required to maintain the vapor temperature at 790°C, which represents the heat losses through the insulation.

The total power delivered to maintain steady state was 455 W. It includes both the power carried by the VCHP (and rejected by the radiator) with the ASC OFF and the 162 W heat losses through the insulation. The difference, roughly 290 W, is the heat rejected by the radiator. It is an approximate value, because the heat losses were measured at 790°C, while the total power was measured at 820°C. It is higher than the GPHS power of 250 W because the radiator was deliberately oversized.

B. Experimental Procedure – "Gravity Aided" and "Against Gravity"

The "gravity aided" tests were carried out with the VCHP in the orientation shown in Fig. 5, where condensate can drain down from the condenser to the evaporator. In the "against gravity" tests, the VCHP was turned upside down. Both the "gravity aided" and "against gravity" tests were carried out in four sequences, B1 through B4. These tests were different from those performed during the preliminary experiment:

1) Sequence B1 evaluated the heat losses through the insulation. The power necessary to reach steady state conditions at 790°C vapor temperature, with no cooling (ASC OFF), was considered as heat losses through the insulation to the ambient.

2) Sequence B2 simulated the ASC ON and VCHP OFF situation. Cooling air was ON (7.6 m/s), and power was increased to approximately 450 W until a new steady state was obtained at the same vapor temperature of 790°C.

3) Sequence B3 simulated the ASC OFF and VCHP ON situation. The cooling air was turned OFF, letting the front move toward the end of the condenser to turn the VCHP ON and reach steady state in the new conditions (vapor temperature around 820°C).

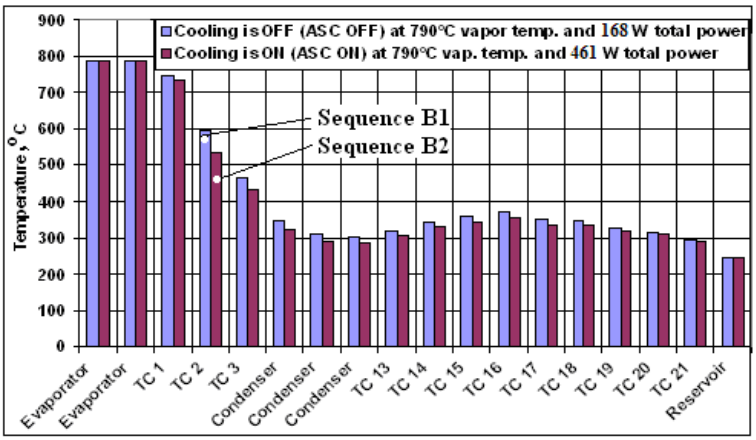

Figure 8. VCHP temperature distributions at the end of sequences B1 and B2 of the "gravity aided" experiment.

4) Sequence B4 simulated the new ASC ON and VCHP OFF situation (restarting the ASC) after the front retracted. The cooling air was turned ON again (7.6 m/s), letting the front retract toward the evaporator to turn the VCHP OFF and reestablish the steady state conditions from sequence B2 (vapor temperature of 790°C). The transient state of the last two sequences, B3 and B4, are discussed later in the paper.

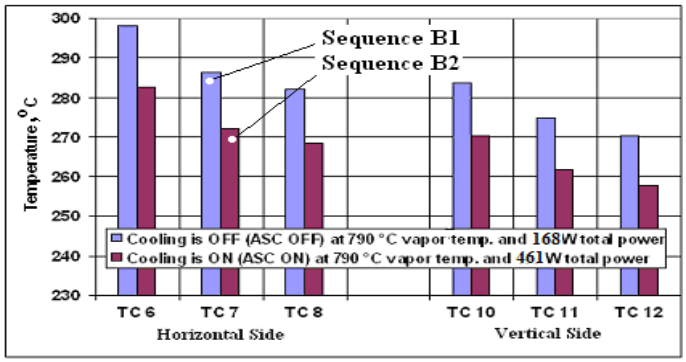

Figure 9. Radiator temperature distributions at the ends of sequences B1 and B2 of the "gravity aided" experiment.

C. "Gravity Aided" Experiment

As mentioned above, the "gravity aided" experiment was carried out very close to the most favorable conditions from a VCHP performance point of view, with the evaporator at the bottom and the reservoir on top. The steady state conditions (reached at the end of each of the four sequences) will be discussed in the first part of this section, while the transient responses (during sequences B3 and B4) will be discussed in the second part of this section.

Figure 8 shows the temperature distributions along the VCHP at the ends of the first two sequences (described above) of the "gravity aided" experiment. It can be observed from sequence B2 that, when cooling is ON (ASC ON), all the temperatures along the VCHP are slightly lower compared to the cooling OFF case, except for the evaporator and reservoir. This is because the heater head is cooler due to the air flow, and this slightly cools the condenser and the connecting tubes. In both sequences, however, the front is located at the exit of the evaporator at a vapor temperature of 790°C and reservoir temperature of 249°C. Heat losses during sequence B1 are 168 W, while total power and air cooling velocity during sequence B2 are 461 W and 7.6 m/s, respectively.

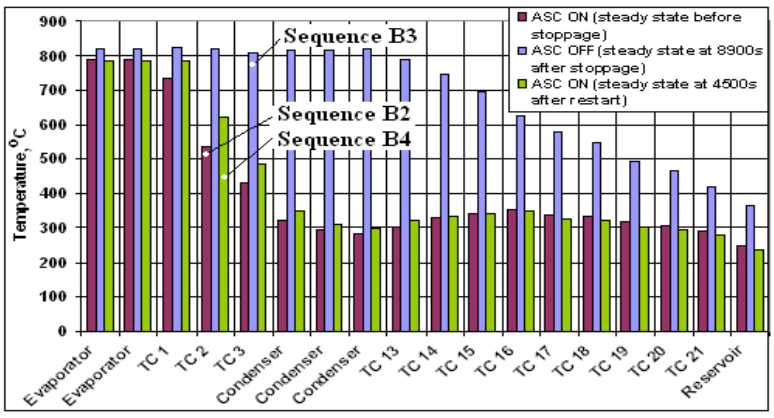

Figure 10. VCHP temperature distributions at the ends of the last three sequences (B2, B3, and B4) of the "gravity aided" experiment.

Figure 9 presents the radiator temperature distributions at the ends (steady state) of the first two sequences of the "gravity aided" experiment. Although the vapor temperatures are the same during these two sequences, the cooled situation (ASC ON) determines lower temperatures on the radiator due to the proximity of the heater head, which now is cooler. This difference yields lower losses for the cooled situation.

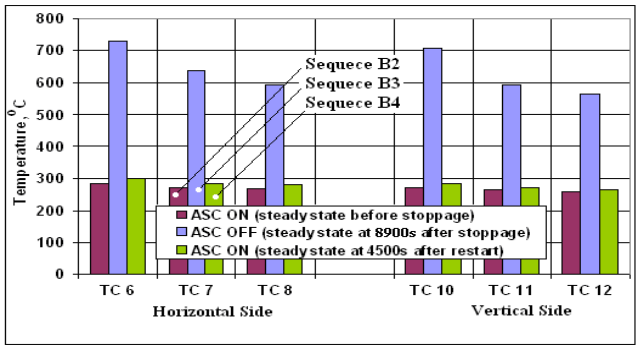

Figure 11. Radiator temperature distributions at the ends of the last three sequences of the "gravity aided" experiment

The temperature distributions at the ends of the last three sequences are shown in Fig. 10 (B2 – ASC ON, B3 – ASC OFF, B4 – ASC ON after restart). During sequence B2, the front was located, under steady state conditions, at the exit of the evaporator for the parameters presented above for Fig. 8. Sequence B3 started when the cooling air was turned OFF. Consequently, the front moved toward the condenser to turn the VCHP ON. It settled under steady conditions at the end of the condenser when the vapor temperature reached an average value of 821°C and the hot reservoir temperature reached 374°C. This was the end of sequence B3. When air cooling was turned ON again (ASC ON after restart – beginning of sequence B4), at the same velocity of 7.6 m/s, the front returned to the evaporator. At the end of sequence B4, the front settled at the exit of the evaporator extension (TC 1) for a 790°C vapor temperature and 241°C cold reservoir temperature. The two temperature distributions, corresponding to the sequences B2 and B4, present noticeable differences. The reservoir temperature is slightly lower for the fourth sequence, allowing the front to settle at TC 1. This rather advanced position of the front determines higher temperatures on the VCHP section between the evaporator and condenser (thermocouples 1 through 4). This difference between the two temperature profiles shows that steady state has not yet been reached.

Radiator temperature profiles for sequences B2, B3, and B4 are presented in Fig. 11. An approximate temperature drop of 90°C between the vapor (820°C) and thermocouple 6 on the radiator can be observed for sequence B3 (ASC OFF and VCHP ON).

The transient VCHP temperature profiles for sequences B3 and B4 are presented in Fig. 12. Sequence B3 (Fig.

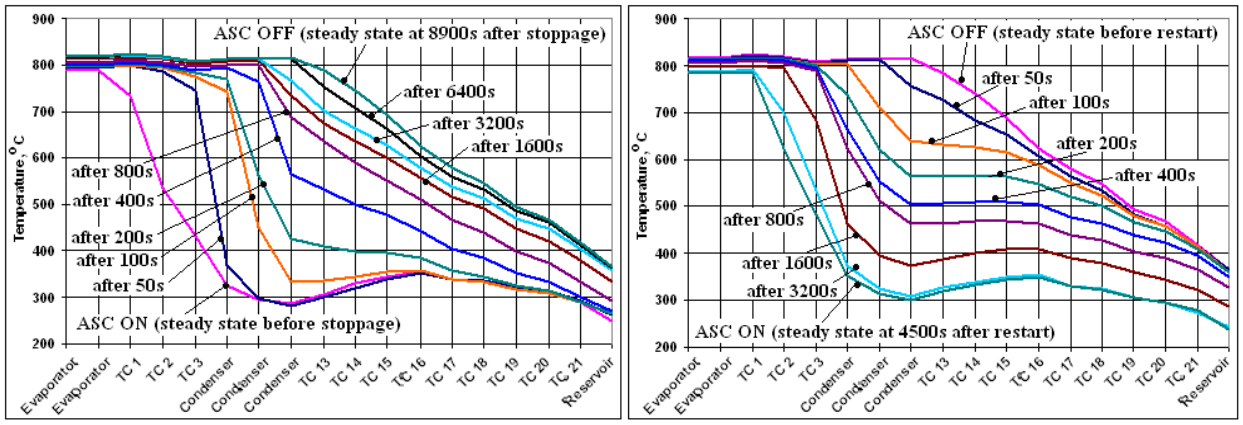

a) **b)**

Figure 12. VCHP temperature distributions during (a) Sequence B3 (ASC OFF, front moves toward the end of the condenser to turn the VCHP ON) and (b) Sequence B4 (ASC ON after restart, front retracts toward

12a), starts with the lowest temperature profile, where the cooling air is active (ASC ON). The evaporator is at 790°C, and all of the heat is going from the heater, through the annular evaporator, and into the cooling air. The radiator is OFF, with temperatures below 300°C. Once cooling is stopped (ASC OFF), the system starts to heat up, and the NCG gas front moves toward the condenser. As it travels up the condenser, heat is transferred to the simulated ASRG wall and then to the ambient by radiation and natural convection.

Sequence B4, shown in Fig. 12b, was run immediately after sequence B3, so the top curves in Figures 12a and 12b are identical. When cooling is turned on (ASC ON), the system gradually cools. The temperature and pressure in the vapor drop, and the NCG front moves back towards the annular evaporator. As expected, the gas front moves at a faster rate in the beginning and slower toward the end of each of the two sequences, as steady state conditions are approached. It can be observed that the front is slower during sequence B3 (VCHP turning ON) than during sequence B4 (VCHP turning OFF). The reason is unclear yet. However, the general transient duration will be compared with the results from the "against gravity" case.

D. "Against Gravity" Experiment

In the "against gravity" case, the VCHP was tested upside down (in a vertical position) with the evaporator above the reservoir (opposite to the "gravity aided" case). The results were generally in agreement with the model, and no VCHP performance drawbacks were observed. Most of the findings and conclusions regarding the VCHP behavior are similar to the previous "gravity aided" case. However, significant reservoir temperature and transient time differences were observed, and we believe that they are related.

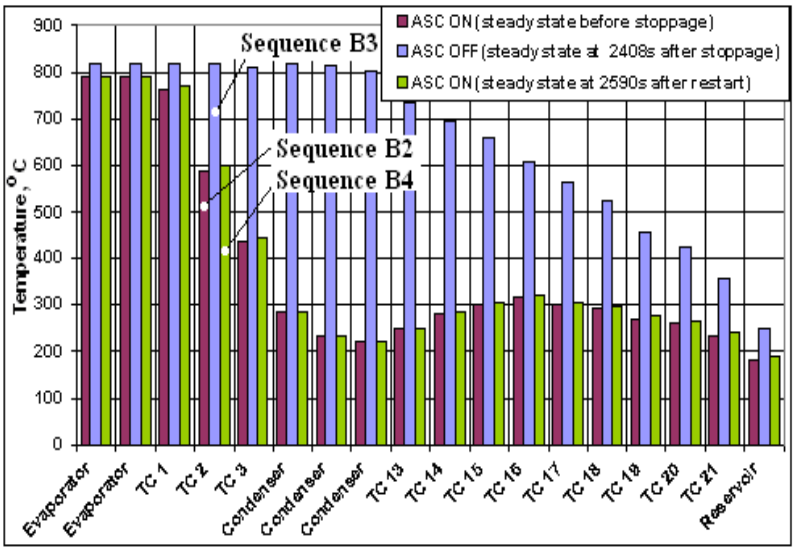

Figure 13. VCHP temperature distributions at the ends of the last three sequences of the "against gravity" experiment.

Temperature distributions at the ends of the last three (B2, B3, and B4) experimental sequences of the "against gravity" case are presented in Fig. 13. The general progression of the sequences is similar to the previous "gravity aided" case. Again, although sequence B4 was considered completed when no noticeable vapor temperature variation around 790°C was detected, a true steady state situation was not

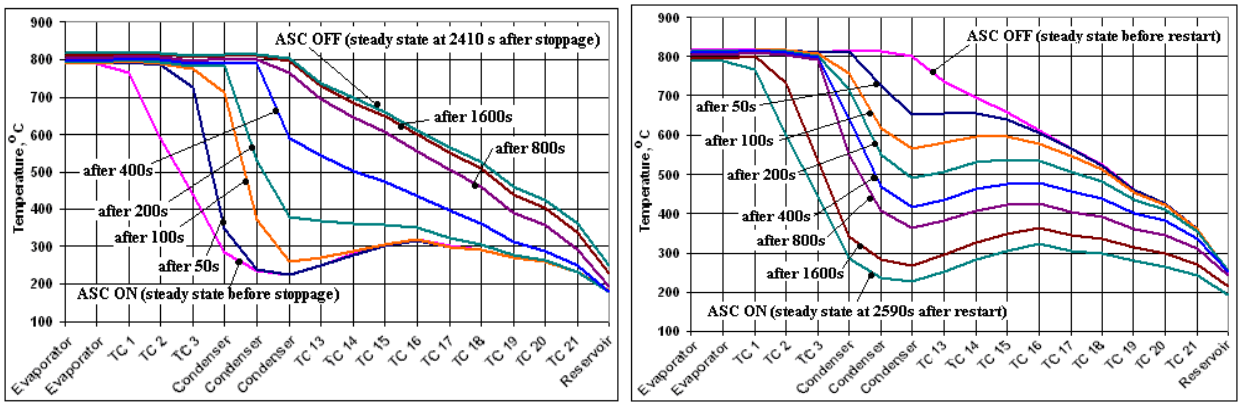

a) **b)**

Figure 14. VCHP temperature distributions during (a) Sequence B3 (ASC OFF, front moves toward the end of the condenser to turn the VCHP ON) and (b) Sequence B4 (ASC ON after restart, front retracts toward the evaporator to turn the VCHP OFF) of the "against gravity" experiment.

reached. The gas front is slightly advanced toward the condenser despite all the VCHP temperatures which are higher (including the reservoir) than those in sequence B2. Table 4 shows a summary of the reservoir temperatures at the ends of sequences B2, B3, and B4 in both "gravity aided" and "against gravity" cases. It can be observed that all reservoir temperatures during the "against gravity" experiment are significantly lower than the corresponding cases of the "gravity aided" experiment.

Table 4. Summary of the reservoir temperatures.

Case	Reservoir Status	Sequence	Temperature [°C]
Gravity Aided	Cold	B2	247
	Hot	B3	366
	Cold	B4	243
Against Gravity	Cold	B2	180
	Hot	B3	250
	Cold	B4	191

Figure 14 shows the details of the transient movement of the gas front (VCHP temperature distributions) during sequences B3 and B4. Similar to the "gravity aided" case, the gas front moves at a faster rate in the beginning of each of the two sequences, slowing down significantly as steady state is approached. In the "against gravity" case, the front moves approximately two times faster in sequence B4 and four times faster in sequence B3 than in the corresponding sequences of the "gravity aided" case. Again, it can be observed that the reservoir is significantly

hotter in the "gravity aided" case than in the "against gravity" case during all sequences. Preliminarily, we believe that the difference between the front velocities in the two cases, "gravity aided" and "against gravity", is due to the difference in reservoir temperatures and their transients. Faster heating of the reservoir may suppress the front movement longer, causing a slower front velocity. In turn, the difference in reservoir temperatures between the two cases may be caused by gravity effects materialized by the following two components:

1) External free convection through the insulation in the "gravity aided" case that causes a faster heating up of the reservoir.
2) Internal buoyancy forces (also in the "gravity aided" case) may also cause a more rapid heating of the reservoir because of the lighter sodium vapor at the reservoir temperatures (see Fig. 15). Sodium vapor can penetrate the front by diffusion (at the temperatures of the front region, sodium is heavier than argon). Once the sodium reaches the colder zones (where it becomes lighter than the argon), the upward motion is buoyancy driven, so the sodium will eventually reach the reservoir and condense. This phenomenon may not happen in the "against gravity" case allowing a lower temperature of the reservoir.

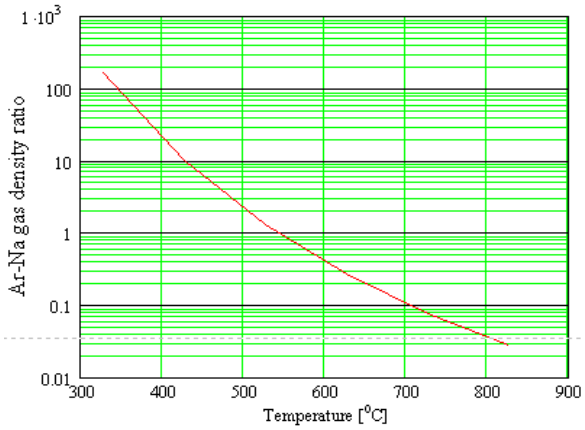

Figure 15. Argon-Sodium gas density ratio as a function of temperature.

To verify this hypothesis, new measurements will be carried out for several VCHP orientations, including horizontal.

IV. Conclusion

The first VCHP prototype for a radioisotope Stirling system has been successfully fabricated and tested. The system has a baseline temperature of 790°C and uses sodium as the working fluid. The experimental results matched the modeling predictions very well for both "gravity aided" and "against gravity" (upside down) working conditions. For the "gravity aided" case and under steady conditions, the front was located at the evaporator exit with a vapor temperature of 790°C for the simulated case of an operating Stirling convertor (cooling was active and the VCHP was off). When the cooling was stopped (simulating a stopped Stirling convertor), the gas front moved and settled at the end of the condenser with an 820°C vapor temperature and turning on the VCHP. This showed a 30°C vapor temperature increase, as designed. When cooling was started again (simulating a restart of the Stirling convertor), the gas front retreated to the evaporator exit to, again, turn off the VCHP and settled at the same initial vapor temperature, 790°C. The VCHP performance was similar for the "against gravity" case. Heat rejected by the radiator was about 270 W for both "gravity aided" and "against gravity" cases.

The only noticeable difference between the results of the two extreme cases ("gravity aided" and "against gravity"), were the reservoir temperature and the front traveling time. The reservoir was significantly hotter in the "gravity aided" case than in the "against gravity" case during both cold (VCHP OFF) and hot (VCHP ON) regimes. Also, the front traveling speed was approximately two to four times higher in the "against gravity" case than in the "gravity aided" case. A preliminary hypothesis is that the difference in the reservoir temperatures and their transients may determine the difference in front velocity between the two cases. In addition, the gravity effects may cause the reservoir temperature differences. The external natural convection through the insulation of the system and internal buoyancy forces on the sodium vapor, which is lighter than the NCG (argon) at the reservoir temperature, may heat the reservoir more in the "gravity aided" case. To verify these hypotheses, additional measurements in different gravity orientations, other than the two extreme cases investigated so far, will be performed.

Acknowledgments

This research was sponsored by NASA Glenn Research Center under Phase II Small Business Innovation Research (SBIR) Contract No. NNC07QA40P. Any opinions, findings, and conclusions or recommendations expressed in this article are those of the authors and do not necessarily reflect the views of the National Aeronautics and Space Administration. Lanny Thieme is the contract technical monitor. We would like to thank Jeff Schreiber and Jim Sanzi of NASA Glenn Research Center, and Jaime Reyes and Michael Welz of Lockheed Martin Space Systems Company for helpful discussions about the Stirling system and the VCHP. Tim Wagner was the technician for the program.

References

[1]Chan, T.S., Wood, J. G. and Schreiber, J. G., "Development of Advanced Stirling Radioisotope Generator for Space Exploration," *NASA Glenn Technical Memorandum* NASA/TM-2007-214806, 2007. http://gltrs.grc.nasa.gov/reports/2007/TM-2007-214806.pdf.

[2]Rosenfeld, J. H., Ernst, D. M., Lindemuth, J. E., Sanzi, J., Geng, S. M., and Zuo, J., "An Overview of Long Duration Sodium Heat Pipe Tests," NASA Glenn Technical Memorandum NASA/TM—2004-212959, 2004. http://gltrs.grc.nasa.gov/citations/all/tm-2004-212959.html